PHYSICAL REVIEW E **93**, 050201(R) (2016)

Light-matter interaction induces a shadow vortex

R. Barboza,[1] U. Bortolozzo,[2] M. G. Clerc,[1] J. D. Davila,[3] M. Kowalczyk,[3] S. Residori,[2] and E. Vidal-Henriquez[4]

[1]*Departamento de Física, FCFM, Universidad de Chile, Casilla 487-3, Santiago, Chile*

[2]*Institut Non Linéaire de Nice, Université de Nice-Sophia Antipolis, CNRS, 1361 Route des Lucioles, 06560 Valbonne, France*

[3]*Departamento de Ingeniería Matemática and Centro de Modelamiento Matemático (UMI 2807 CNRS), FCFM, Universidad de Chile, Casilla 170 Correo 3, Santiago, Chile*

[4]*Max Planck Institute for Dynamics and Self-Organization, Am Fassberg 17, D-37077 Göttingen, Germany*

(Received 15 February 2016; published 16 May 2016)

By sending a light beam on a homeotropic nematic liquid-crystal cell subjected to a voltage with a photosensitive wall, a stable matter vortex can be induced at the center of the beam. When the applied voltage is decreased, the vortex disappears from the illuminated region; however, the system shows a stationary molecular texture. Based on a forced Ginzburg-Landau amplitude equation, we show that the vortex with a core of exponentially suppressed amplitude always remains in a shadow region below instability threshold and that the observed texture is induced by its phase distribution. This is a different type of vortex phase singularity solution. Numerical simulations and experimental observations show a quite fair agreement.

DOI: 10.1103/PhysRevE.93.050201

In two-dimensional systems, dissipative vortices are described by the complex Ginzburg-Landau equation (CGLE), which has universal character and describes such different systems as fluids, superfluids, superconductors, liquid crystals, granular media, magnetic media, and optical dielectrics, to mention a few [1–3]. Vortices occur in complex fields and can be identified as topological defects, that is, pointlike singularities which locally break the symmetry. They exhibit zero intensity at the singular point with a phase spiraling around it. The topological charge is assigned by counting the number of spiral arms in the phase distribution, while the sign is given by the sense of the spiral rotation.

Liquid crystals with negative anisotropic dielectric constant and homeotropic anchoring are a natural physical context where dissipative vortices are observed [4,5]. The nematic liquid-crystal phase is characterized by rod-shaped molecules that have no positional order but tend to point in the same direction. The state of the nematic liquid crystal is described by a vector—the director $\vec{n}$—which accounts for the molecular order. When a homogeneous layer of nematic liquid crystal is subjected to a low frequency electric field along the director, the molecules will tend to align perpendicularly to the electric field if the dielectric anisotropy is negative; this is in order to minimize the dipolar interaction of the molecules and the electric field [5]. Due to the competing behavior of the torque generated by the applied field and the intrinsic elastic torque generated by the liquid-crystalline medium, an effective reorientation will occur when the electric torque overcomes the elastic one. Thus, over the critical voltage at which this imbalance occurs, i.e., the *Fréederickz transition voltage*, the molecules will align towards the plane normal to the electric field but in random directions, causing the emergence of dissipative defects, which will tend to disappear with the aim of establishing a new molecular orientation that minimizes the energy of the system. This effect can be easily observed experimentally in geometries where the liquid crystal is confined between two conductive glass plates, treated to promote orthogonal, so-called homeotropic, alignment of the molecules at the interface between the liquid crystal and the glass plate. The electric field can be applied to the liquid-crystal layer via a low frequency voltage through the inner transparent conductive coating of the glass plates. Dissipative vortices are known in this context as umbilical defects [4]. Two types of stable vortices are observed. They have opposite charges and are characterized by being attracted to (repulsed from) the opposite (identical) topological charge. Note that the defects observed in this context are strongly dissipative, compared to those observed in magnetic systems, superfluids, superconductors, and Bose-Einstein condensates. Recently, by exploiting reorientational nonlinearities in the nematic liquid-crystal layer of an optically addressable liquid-crystal cell, the so-called liquid-crystal light valve (LCLV), it has been shown that spontaneous, stable matter vortices can be induced at the chosen location [6,7]. This is accomplished by sending light beams onto a homeotropic nematic liquid-crystal cell subjected to a voltage with a photosensitive wall. Figure 1 shows a schematic representation of the experimental setup and the typical vortex observed using linear crossed polarizers. When the voltage V_0 applied to the cell is decreased, the vortex disappears from the illuminated region; however, the system shows a stationary molecular texture that is characterized by dark lines separating different lobes of molecular orientations [cf. Fig. 1(c)]. The induced voltage in the illuminated area is above the threshold, i.e., *Fréederickz tension*, necessary for the molecules to reorient. The unilluminated area, i.e., *shadow region*, is characterized by having the applied voltage lower than the critical threshold. The texture deformation revealed by the lines of zero intensity intersecting at the boundary of the illuminated region identifies the presence of a shadow vortex.

The stability properties and dynamical evolution of the vortices are associated with their topological nature. Therefore, the mechanisms through which these solutions disappear or self-organize in extended systems are open questions. The aim of this Rapid Communication is to explain the mechanism of disappearance of a vortex and the emergence of a reorientation domain as a result of light-matter interaction in a liquid-crystal light cell with a photosensitive wall. Based on a forced Ginzburg-Landau amplitude equation that describes the system under study, we show that the observed texture is induced by the phase of the vortex with an exponentially small

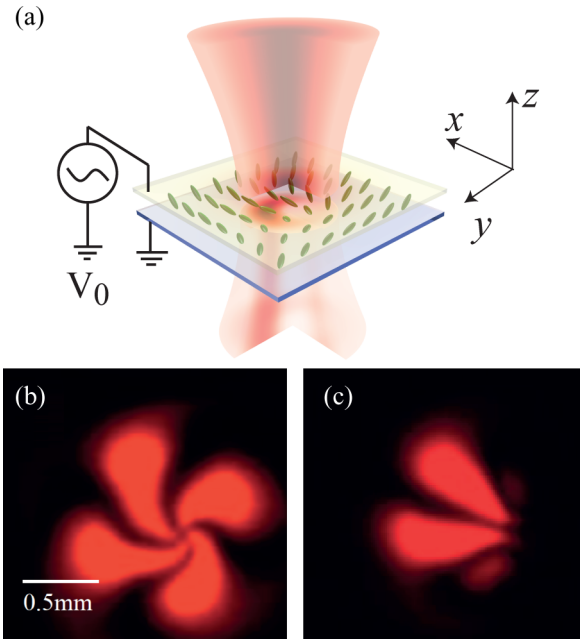

FIG. 1. (a) Schematic setup for vortex induction; a light beam is incident on the photoconductive side of the LCLV. (b),(c) Intensity profiles measured using linear crossed polarizers for a large ($V_0 = 18$ V) and a small ($V_0 = 17$ V) voltage, respectively. The presence of a shadow vortex is revealed in (c) by the lines of zero intensity intersecting at the boundaries of the illuminated region.

amplitude located in a region below the instability threshold, i.e., the shadow region. The shadow vortex is a different type of phase singularity solution. Numerical simulations and experimental observations show a quite fair agreement.

To describe the dynamics of the illuminated liquid-crystal light valve filled with a negative dielectric nematic liquid crystal and homeotropic anchoring, we consider a model in the vicinity of the Fréedericksz transition, a limit where analytical results are accessible as nematic liquid-crystal molecules are weakly tilted from the longitudinal axis $\hat{z}$ and backflow effects can safely be neglected. The dynamical equation for the molecular director $\vec{n}(\vec{r},t)$ reads [5]

$$\begin{aligned}\gamma\,\partial_t\vec{n} = {} & K_3[\nabla^2\vec{n} - \vec{n}(\vec{n}\cdot\nabla^2\vec{n})] \\ & + (K_3 - K_1)[\vec{n}(\vec{n}\cdot\vec{\nabla})(\vec{\nabla}\cdot\vec{n}) - \vec{\nabla}(\vec{n}\cdot\vec{\nabla})] \\ & + 2(K_2 - K_3)\{(\vec{n}\cdot\vec{\nabla}\times\vec{n})[\vec{n}(\vec{n}\cdot\vec{\nabla}\times\vec{n}) - \vec{\nabla}\times\vec{n}] \\ & + \vec{n}\times\vec{\nabla}(\vec{n}\cdot\vec{\nabla}\times\vec{n})\} + \epsilon_a(\vec{n}\cdot\vec{E})[\vec{E} - \vec{n}(\vec{n}\cdot\vec{E})], \quad (1)\end{aligned}$$

where γ is the relaxation time, ϵ_a is the anisotropic dielectric constant ($\epsilon_a < 0$), and $\{K_1, K_2, K_3\}$ are, respectively, the splay, twist, and bend elastic constants of the nematic liquid crystal. Under uniform illumination, $\vec{E} = [V_0 + \alpha I]/d\ \hat{z}$, where V_0 is the voltage applied to the LCLV, d is the thickness of the cell, I is the intensity of the illuminating light beam, and α is a phenomenological dimensional parameter that describes the linear response of the photosensitive wall [8]. The homeotropic state, $\vec{n} = \hat{z}$, undergoes a stationary instability for critical values of the voltage which match the effective Fréedericksz transition threshold $V_{FT} = \sqrt{-K_3\pi^2/\epsilon_a} - \alpha I$.

Illuminating the liquid-crystal light valve with a Gaussian beam induces a voltage drop with a bell-shaped profile across the liquid-crystal layer, and higher in the center of the illuminated area. The electric field within the sample takes the form [7]

$$\vec{E} = E_z\hat{z} + E_r\hat{r} \equiv \frac{[V_0 + \alpha I(r)]}{d}\hat{z} + \frac{z\alpha}{d}I'(r)\hat{r}, \quad (2)$$

where r is the radial coordinate centered on the beam, $\hat{r}$ is the unitary radial vector, $I(r)$ is the intensity of the Gaussian light beam, $I(r) = I_0 e^{-r^2/2\omega^2}$, I_0 is the peak intensity, and ω is the waist of the light beam.

Considering the intensity of the light beam as small enough and close to the Fréedericksz transition, one can use the following ansatz for the amplitude of the critical spatial mode [7]:

$$\vec{n}(r,\theta,z,t) \approx \begin{pmatrix} u(r,\theta,t)\sin\left(\frac{\pi z}{d}\right) \\ w(r,\theta,t)\sin\left(\frac{\pi z}{d}\right) \\ 1 - \frac{1}{2}(u^2+w^2)\sin^2\left(\frac{\pi z}{d}\right) \end{pmatrix}. \quad (3)$$

Introducing the above ansatz in the director equation, integrating in the z coordinate over the sample thickness, and considering the complex amplitude $A \equiv (u + iw)$, after straightforward calculations one obtains the forced Ginzburg-Landau equation [6,7],

$$\gamma\,\partial_t A = \mu A - a A|A|^2 + K\nabla_\perp^2 A + \delta\partial_{\eta\eta}\bar{A} + bI'(r)e^{i\theta}, \quad (4)$$

where $\mu(r) \equiv -K_3k^2 - \epsilon_a E_z^2(r)$ is the bifurcation parameter, $a \equiv -(K_3k^2/4 + 3\epsilon_a E_z^2/4) > 0$, $k \equiv \pi/d$, $b \equiv 2\epsilon_a\alpha V_0/d\pi$, $\partial_\eta \equiv \partial_x + i\,\partial_y$, $K \equiv (K_1 + K_2)/2$, and $\delta \equiv (K_1 - K_2)/(K_1 + K_2)$ accounts for the elastic anisotropy. Note that in the ansatz [Eq. (3)], higher order nonlinear terms in amplitude A have been neglected.

Neglecting the anisotropy ($K_1 = K_2 = K_3$ and $\delta = 0$) and considering homogeneous illumination ($I = I_0$), the above model reduces to the well-known Ginzburg-Landau equation with real coefficients, which admits stable dissipative vortex solutions with topological charge ± 1 [1,10]. However, due to their microscopic constituents (rod-shaped molecules), liquid crystals are anisotropic materials, and thus, in general, $K_1 \neq K_2 \neq K_3$. When the anisotropy is taken into account ($\delta \neq 0$), this generates a symmetry breaking of vortex solutions with different topological charge [9]. This anisotropic amplitude equation adequately describes the dynamics of the nematic umbilical defects.

Taking into account inhomogeneous illumination and anisotropy, the system is described by Eq. (4). The last term on the right-hand side is an external forcing generated by the inhomogeneous radial electric field. Such forcing term is responsible for inducing a matter vortex with positive charge at the center of the applied Gaussian beam [6]. The anisotropic term is responsible for slight rotation of the matter vortex; also due to this term a vortex of positive charge is energetically preferred by the system [9]. Figure 2 shows a typical vortex solution obtained from numerical simulations of the model given by Eq. (4). Notice that the nullcline field $\psi(x,y,t) \equiv \mathrm{Re}(A)\mathrm{Im}(A)$ adequately realizes the experimental observations using linear crossed polarizers. The numerical simulations were conducted considering a triangular finite

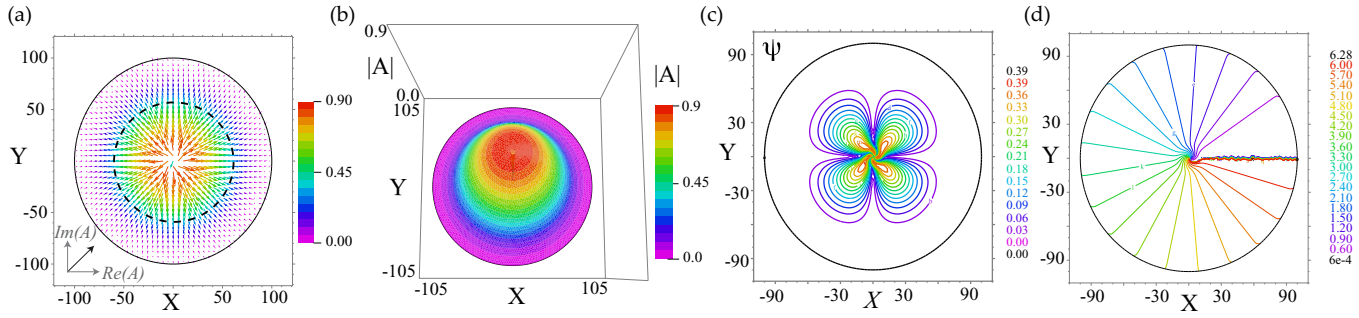

FIG. 2. Induced vortex obtained from numerical simulations of the forced Ginzburg-Landau equation (4) with $\mu(r) = -0.2 + e^{-r^2/2000}$, $a = 1$, $b = -5$, $I'(r) = -re^{-r^2/2000}/1000$, and $\delta = 0.7$. (a) Vector representation of the complex amplitude $A(x,y)$, with the horizontal and vertical components corresponding, respectively, to the real and imaginary parts of A. The dashed circumference stands for the illuminated area, which corresponds to the region with positive μ. (b) Tridimensional graph of the magnitude of the complex amplitude $A(x,y)$. (c) Contour plot of the nullcline field $\psi(x,y) = \mathrm{Re}(A)\mathrm{Im}(A)$. (d) Phase field of the complex amplitude $A(x,y)$.

element code with adaptive spatial and temporal steps, and a simulation box of dimensions 100×100 with Neumann boundary condition. Hence, model (4) adequately describes the observed dynamics of light-matter interaction in a liquid-crystal light cell with a photosensitive wall [6,7].

When the voltage is decreased, it crosses a critical value and the vortex in the center of the illuminated region becomes unstable. As a result, it moves from the illuminated region towards the unilluminated region and, at the end, the vortex is located in the region below the Fréederickz threshold—we call this type of phase singularity a shadow vortex. Figure 3 shows different properties of the shadow vortex that make it distinct from the standard vortex. Note that the shadow vortex is positioned near the region where the bifurcation parameter changes sign. This is easy to discern by analyzing the phase of the amplitude A [cf. Fig. 3(c)]. However, experimental derivation of the phase using the polarimetry technique in a region where the amplitude is exponentially small becomes difficult if possible. Therefore, the orientation domain of the field A in the illuminated region is completely determined by the vortices in the shadow region [cf. Fig. 3(a)]. Because the shadow vortex is located in the region of exponentially suppressed amplitude [see Fig. 1(d)], it is difficult to detect it position from the magnitude of the amplitude. At the same time, the form of the nullcline field obtained numerically [cf. Fig. 3(b)], which is quite similar to the one observed experimentally [cf. Fig. 1(c)], clearly indicates the shadow vortex center. Notice that due to forcing, the inhomogeneous solution without topological charge is not a solution of the system.

When the bifurcation parameter is positive and inhomogeneous, $\mu(r)$, and without forcing ($b = 0$), it is known that the vortex moves down the gradient of this parameter to minimize the system energy [10]. The corresponding topologically trivial solution is called corner layer [11]. Tuning the forcing on induces the vortex with positive charge at the center of the light beam. The balance between these effects determines whether the position of the vortex is in the bright region or in the dark region. By increasing the voltage applied to the sample, the shadow vortex becomes unstable and moves to the illuminated region and positions itself at the center of the light beam—the local profile of this phase singularity is that of the standard vortex.

To understand the dynamics of these phase singularities, we have considered the equivalent equation in one dimension,

$$\partial_t u = (\mu_0 + \beta e^{-x^2/\omega^2})u - u^3 + \partial_{xx}u + \alpha x e^{-x^2/\omega^2}, \qquad (5)$$

where $u(x,t)$ is a one-dimensional order parameter, $\mu_0 < 0$ is a control parameter, β stands for the intensity of the inhomogeneous linear parameter and satisfies $\beta + \mu_0 > 0$, ω is the width of the Gaussian, and α is the intensity of the forcing. For $\beta = \alpha = 0$, the previous model (5) corresponds to the real Ginzburg-Landau equation or the overdamped

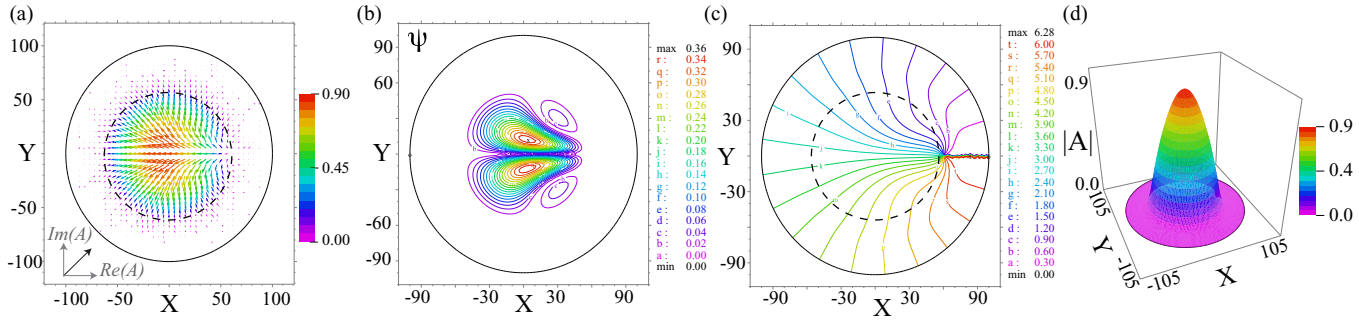

FIG. 3. Shadow vortex obtained from numerical simulations of the forced Ginzburg-Landau equation (4) with $\mu(r) = -0.2 + e^{-r^2/2000}$, $a = 1$, $b = -0.02$, $I'(r) = -re^{-r^2/2000}/1000$, and $\delta = 0.1$. (a) Vector representation of the complex amplitude $A(x,y)$. The dashed circumference stands for the illuminated area, which corresponds to the region with positive μ. (b) Contour plot of the nullcline field $\psi(x,y)$. (c) Phase field of the complex amplitude $A(x,y)$. (d) Tridimensional graph of the magnitude of the complex amplitude $A(x,y)$.

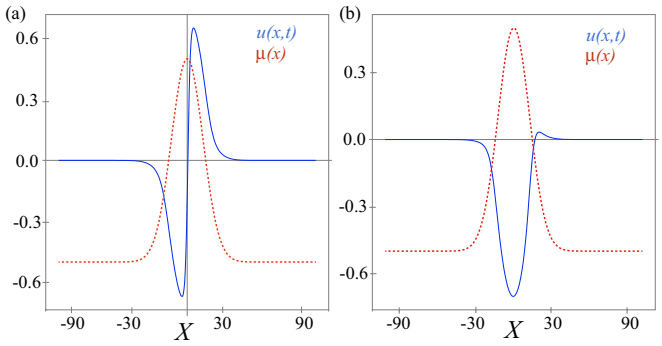

FIG. 4. Induced kinks obtain from numerical simulation of the one-dimensional forced real Ginzburg-Landau equation (5) with $\mu_0 = -0.5$, $\omega = 17{,}32$, and $\beta = 1.0$. (a) Standard kink with $\alpha = 0.005$. (b) Shadow kink with $\alpha = 0.002$. The solid and the dashed curves account for the stationary solution of the scalar field $u(x)$ and the inhomogeneous bifurcation parameter $\mu(x)$.

ϕ^4 model. Topologically nontrivial solutions of Eq. (5) are kinks—they correspond to vortex solutions in Eq. (4). When the kinks are spatially monotone increasing (decreasing), they are positively (negatively) charged. The inhomogeneous linear term (proportional to β) causes the kink to move in the direction of its gradient and its effect is similar to that in the two-dimensional equivalent. On the other hand, the forcing term (proportional to α) tends to generate a kink that is positioned at the origin. Then, the superposition of these two terms—when α is large enough—must generate a kink at the origin, i.e., *standard kink*. Figure 4(a) shows the typical standard kink obtained from numerical simulations of model (5). When α is decreased and exceeds a critical value, the standard kink becomes unstable and begins to move to the region where the linear parameter $\mu(x)$ is negative and is finally positioned in the corner region. Figure 4(b) shows the observed shadow kink. Notice that the core of the shadow kink has an exponentially suppressed amplitude. Due to forcing, the system always has a solution with at least one zero (topological solution). Furthermore, the observed stationary kinks are locally spatially growing, which is consistent with the two-dimensional observations where induced vortices only have positive topological charge. Therefore, the shadow vortices and kinks result from the balance between the forcing and the drag force caused by the inhomogeneous parameter μ. When μ changes sign, the drag force is weaker, and the equilibrium position of defects tends to be located close to the zero level set of μ as seen in one and two dimensions.

Conclusions. By using a nematic liquid crystal in a homeotropic light-valve geometry with optical forcing, we observe experimentally and explain theoretically a different type of phase singularity solution, called the shadow vortex, which is located in a region close to but below the instability threshold, and with a core of exponentially suppressed amplitude. From an experimental point of view, this solution can only be identified by means of its trace—molecular orientations—which it makes in the illuminated region. Considering models in one and two dimensions, we show that the shadow defects are a generic behavior. Since the direction of the molecules and hence the phase of the defect corresponds to the optical axis of an optically anisotropic medium, it is expected that the light beam emerging through this region acquires a Pancharatnam-Berry phase as a result of the shadow vortex, in analogy to similar effects occurring either in q plates [12] or in subwavelength dielectric grating phase plates [13]. Recently, in Ref. [14], using self-induced vortex defects in a liquid-crystal light valve, the realization of programmable optical vortices lattices with arbitrary configuration in space has been demonstrated. The role of shadow vortices can be critical to understand the emergence and disappearance of these lattices. The possibility of tuning vortices between the illuminated and shadow region may allow new applications in astronomy, image processing, manipulable optical tweezers, quantum computation, and data transmission.

M.G.C., R.B., M.K., and J.D.D. acknowledge funding from the FONDECYT Projects No. 1150507, No. 3140577, No. 1130126, and No. 1130360, respectively. M.K. and J.D.D were partially supported by BASAL project CMM, Universidad de Chile.

[1] L. M. Pismen, *Vortices in Nonlinear Fields* (Oxford Science, New York, 1999).

[2] E. Sandier and S. Serfaty, *Vortices in the Magnetic Ginzburg-Landau Model* (Springer Science & Business Media, Boston, 2008).

[3] F. Bethuel, H. Brezis, and F. Helein, *Ginzburg-Landau Vortices* (Springer Science & Business Media, New York, 2012).

[4] S. Chandrasekhar, *Liquid Crystals* (Cambridge University Press, Cambridge, 1992).

[5] P. G. de Gennes and J. Prost, *The Physics of Liquid Crystals*, 2nd ed. (Oxford Science/Clarendon, Oxford, 1993).

[6] R. Barboza, U. Bortolozzo, G. Assanto, E. Vidal-Henriquez, M. G. Clerc, and S. Residori, Vortex Induction via Anisotropy Stabilized Light-Matter Interaction, Phys. Rev. Lett. **109**, 143901 (2012).

[7] R. Barboza, U. Bortolozzo, M. G. Clerc, S. Residori, and E. Vidal-Henriquez, Optical vortex induction via light-matter interaction in liquid-crystal medial, Adv. Opt. Photon. **7**, 635 (2015); Light-matter interaction induces a single positive vortex with swirling arms, Philos. Trans. R. Soc. A **372**, 20140019 (2014).

[8] S. Residori, Patterns, fronts and structures in a liquid-crystal-light-valve with optical feedback, Phys. Rep. **416**, 201 (2005).

[9] M. G. Clerc, E. Vidal-Henriquez, D. Davila, and M. Kowalczyk, Symmetry breaking of nematic umbilical defects through an amplitude equation, Phys. Rev. E **90**, 012507 (2014).

[10] L. M. Pismen, *Patterns and Interfaces in Dissipative Dynamics* (Springer Series in Synergetics, Berlin-Heidelberg, 2006).

[11] N. D. Alikakos, P. W. Bates, J. W. Cahn, P. C. Fife, G. Fusco, and G. B. Tanoglu, Analysis of a corner layer problem in anisotropic interfaces, Discrete Contin. Dyn. Syst. Ser. B **6**, 237 (2006).

[12] L. Marrucci, C. Manzo, and D. Paparo, Optical Spin-to-Orbital Angular Momentum Conversion in Inhomogeneous Anisotropic Media, Phys. Rev. Lett. **96**, 163905 (2006); Pancharatnam-Berry phase optical elements for wave front shaping in the visible domain: Switchable helical mode generation, Appl. Phys. Lett. **88**, 221102 (2006).

[13] G. Biener, A. Niv, V. Kleiner, and E. Hasman, Formation of helical beams by use of Pancharatnam–Berry phase optical elements, Opt. Lett. **27**, 1875 (2002).

[14] R. Barboza, U. Bortolozzo, G. Assanto, E. Vidal-Henriquez, M. G. Clerc, and S. Residori, Harnessing Optical Vortex Lattices in Nematic Liquid Crystals, Phys. Rev. Lett. **111**, 093902 (2013).